CENTRIFUGE TESTING OF BRIDGE PIERS ON CAISSON FOUNDATIONS SUBJECTED TO STRONG GROUND MOTIONS

Domenico Gaudio[1], Gopal Santana Phani Madabhushi[2], Sebastiano Rampello[1] and Giulia Viggiani[2]
[1]*Sapienza University of Rome*
domenico.gaudio@uniroma1.it, *sebastiano.rampello@uniroma1.it*

[2]*University of Cambridge*
mspg1@cam.ac.uk, *gv278@cam.ac.uk*

Abstract

Consideration of the instantaneous bearing capacity of caisson foundations supporting bridge piers and subjected to strong ground motions can lead to a substantial optimisation in caisson design and major cost savings. In the framework of the newly-emerging paradigm of *Capacity Design* extended to geotechnical systems, temporary attainment of limit conditions may be permitted provided that the resulting permanent displacements are smaller than a given threshold value. To validate this new design approach, the seismic performance of caisson foundations was assessed through dynamic centrifuge tests performed on reduced-scale models at the Schofield Centre, University of Cambridge. In this paper, some results obtained in two out of the three tests that were carried out are presented, where a caisson-pier-deck system embedded in a typical alluvial deposit was subjected to a series of earthquakes of increasing intensity. In the two tests at hand, a soft and very soft clay layer was reproduced, so as to either avoid or induce the attainment of the plastic soil behaviour. It is shown that both yielding and failure of the layer of very soft clay limit the inertial forces transmitted to the superstructure, thus validating the design approach which has been taken as a reference in this study and in previous numerical analyses. However, the beneficial effect of soil inelastic and hysteretic behaviour implies the accumulation of permanent rotation of the pier, which increases with earthquake intensity.

1. Introduction

The attainment of plastic mechanisms developing in the foundation soils can hardly be avoided in the presence of strong ground motions. However, current code provisions do not allow the soil-foundation system to fall in the elastic-plastic regime, while requesting that any plastic hinges develop in the superstructure. Even if there are good reasons for this choice (*e.g.,* post-earthquake inspection of the foundation is usually unfeasible), this design concept requires some overstrength factors to be applied in the foundation design, thus introducing a sort of overdesign (Gazetas, 2015). Moreover, sometimes this approach turns out to be even dangerous for the superstructure, as this may be subjected to a high ductility demand (Sakellariadis *et al.,* 2020). Therefore, plastic mechanisms occurring in the foundation soils may be even promoted to limit the inertial forces transmitted to the superstructure, thus leading to substantial cost savings when either designing or retrofitting the structures at hand. However, the beneficial role of this design procedure has to be verified by limiting the displacements and rotations experienced by the structure during and at the end of the seismic event.

Recently, Gaudio and Rampello (2019, 2021) have shown that the above-mentioned design concept can be successfully applied when conceiving caisson foundations supporting bridge piers. As the results were obtained by performing numerical analyses only (3D FE simulations), an experimental validation was deemed necessary: hence, dynamic centrifuge tests on reduced-scale models were recently carried out at the Schofield Centre, University of Cambridge, whose results are shown and discussed in this paper. Fig. 1 shows the problem layout, in which a cylindrical caisson foundation of diameter D = 8 m and slenderness ratio H/D = 1 is embedded in a typical alluvial deposit, made by a thin sand layer (H_1 = 3 m) underlain by a soft clay deposit (H_2 = 14 m).

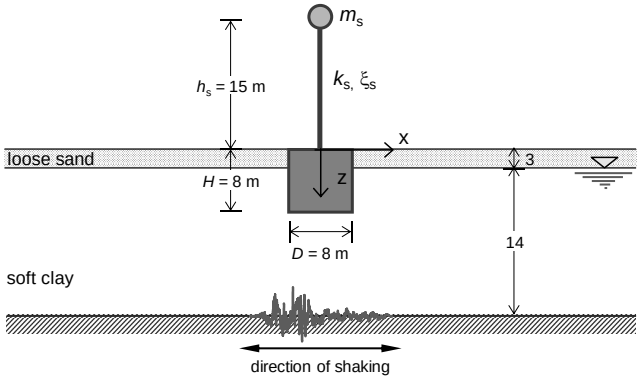

Fig 1. Schematic layout of the problem in prototype scale (dimensions in m)

The water table is located at the sand-clay contact and the pore water pressure regime is hydrostatic. The pier is represented by a Single Degree of Freedom (SDoF) system, characterised by a height h_s = 15 m, while its mechanical properties (lumped mass m_s and stiffness k_s) were back-calculated so as to provide a given weight and fundamental period. The seismic input is applied in terms of a horizontal acceleration time history at the bedrock depth (z = 17 m), here assumed as infinitely rigid and therefore acting as a fully-reflecting boundary.
The schematic layout considered in the centrifuge is not exactly the same as in the numerical analyses: nonetheless, the experimental layout allowed to validate the applicability of the numerical results to different soil-caisson-pier configurations.

2. Experimental setup

A reduced-scale model was produced to simulate the problem layout on the Turner beam centrifuge of the Schofield Centre at University of Cambridge, UK. The centrifuge model was prepared and spun at a nominal centrifugal acceleration of 60*g*.
The model container used was the most recent Equivalent Shear Beam (ESB) container (Brennan and Madabhushi, 2002). The caisson foundation was simulated through a hollow aluminium cylinder topped by two circular aluminium plates, while the pier was modelled using an aluminium rod with a squat brass cylinder at the top to reproduce the mass of the deck. At model scale, the caisson is characterised by a diameter of 133 mm, equal to its depth, while the pier height is equal to 250 mm (Fig. 2). The hole into the caisson foundation was introduced so as to reproduce the mass of a concrete caisson ($m_{caisson}$ = 4.700 kg, corresponding to 1024.8 Mg at prototype scale), while the superstructure is reproduced by the brass mass m_{deck} = 0.900 kg (194.4 Mg) and the pier, the latter characterised by a mass m_{pier} = 0.665 kg (143.6 Mg) and a bending stiffness EI = 2.37 kN·m^2 (30.7 GN·m^2). Hostun sand HN31, available at the Schofield Centre, was glued on the lateral surface of the caisson foundation to reproduce the roughness of the soil-concrete contact (Fig. 3a).
The soil deposit was produced in two steps. First, the clay slurry was prepared by mixing speswhite kaolin clay powder and de-aired water in 1:1.30 ratio, and then the slurry was poured into the ESB box. Two different profiles of undrained shear strength s_u were targeted, both slightly increasing with depth, as for soft clays, and with average values equal to about 45 kPa (test DG01) and 10 kPa (DG03). Fig. 3b shows the undrained shear strength profiles measured performing a *T-bar* test at 60*g*. The desired profiles were obtained via a combination of 1D loading and hydraulic consolidation by suction-induced seepage (Garala and Madabhushi, 2019). After consolidating, the clay surface was trimmed to obtain the desired depth of 233 mm (Fig. 2) and the instrumentation was inserted in the model. The structure was then installed and the clay was covered with a loose sand layer (relative density D_R = 40 %). The instrumentation includes two *far-field* alignments of miniature Pore Pressure Transducers (*PPTs*, $P_{1\text{-}4}$ in Fig. 2) and piezo-electric accelerometers ($p_{1\text{-}6}$): two piezo-electric accelerometers were also installed at the outer base of the ESB container to record the applied seismic

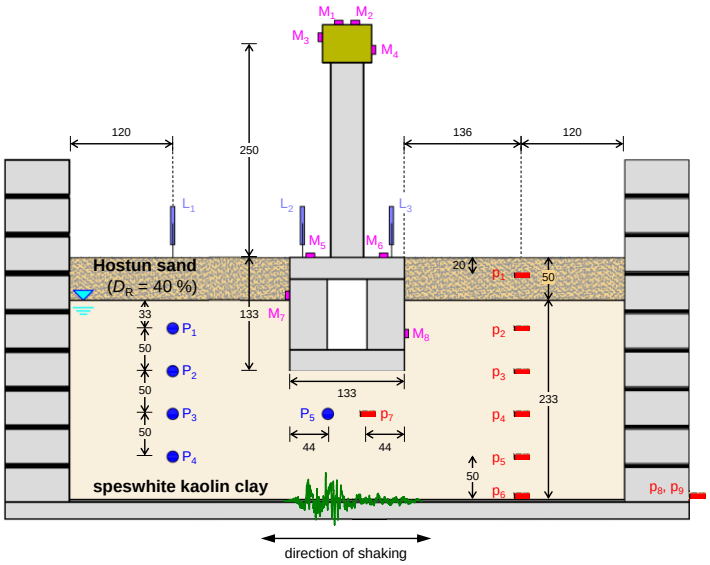

Fig 2. Cross-sectional view of the centrifuge model (dimensions in mm)

input ($p_{8\text{-}9}$), while *PPT* P_5 and piezo-electric accelerometer p_7 were installed beneath the caisson base. Horizontal and vertical acceleration time histories were recorded by Micro-Electro-Mechanical-Systems (*MEMs*) glued on the brass mass ($M_{1\text{-}4}$) and on the caisson ($M_{5\text{-}8}$), whereas the average settlement and rigid rotation of the caisson were measured using two Linear Variable Differential Transformers *LVDTs* ($L_{2\text{-}3}$). Another *LVDT* (L_1) was installed at the clay surface along the *far-field* alignment to record vertical displacements.

Two tests are discussed in this paper, namely DG01 and DG03, the former with the caisson-pier system resting on the stronger clay, the latter on the weaker clay. In both tests, the system was subjected to several real and sinusoidal seismic inputs. Here the results obtained applying the seismic input recorded during the destructive Christchurch (2011) earthquake are discussed; its amplitude was scaled to obtain a weak ($a_x{}^{inp}{}_{max} = 0.030g$, Fig. 4a), a moderate ($a_x{}^{inp}{}_{max} = 0.102g$, Fig. 5a), and a strong ($a_x{}^{inp}{}_{max} = 0.216g$, Fig. 6a) version of the seismic record. The first and the third inputs were applied to the base of the weak clay (DG03), while the second one to the base of the stronger clay (DG01), so as to study the influence of the seismic intensity on the system performance. The ground motions were imposed at the base of the ESB box through the servo-hydraulic shaker described by Madabhushi *et al*. (2012).

3. Seismic performance of the soil-caisson system

In the framework of Performance-Based Design (PBD), the system performance was evaluated through some performance indexes, such as the peak and permanent values of the dimensionless deck drift, u_{rel}/h_s, and the peak bending moment acting at the base of the pier, M_s. The drift is defined as

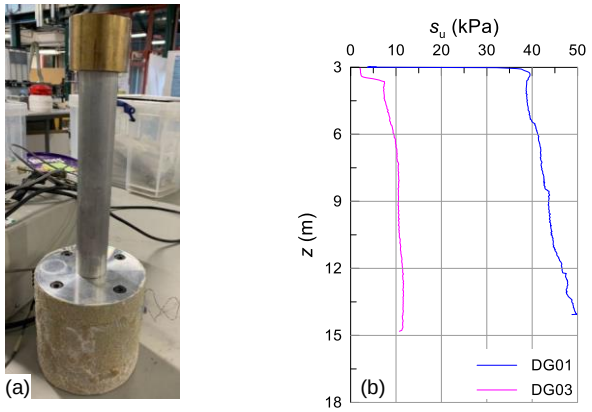

Fig 3. (a) System considered in the centrifuge test DG01-DG03; (b) undrained shear strength profiles

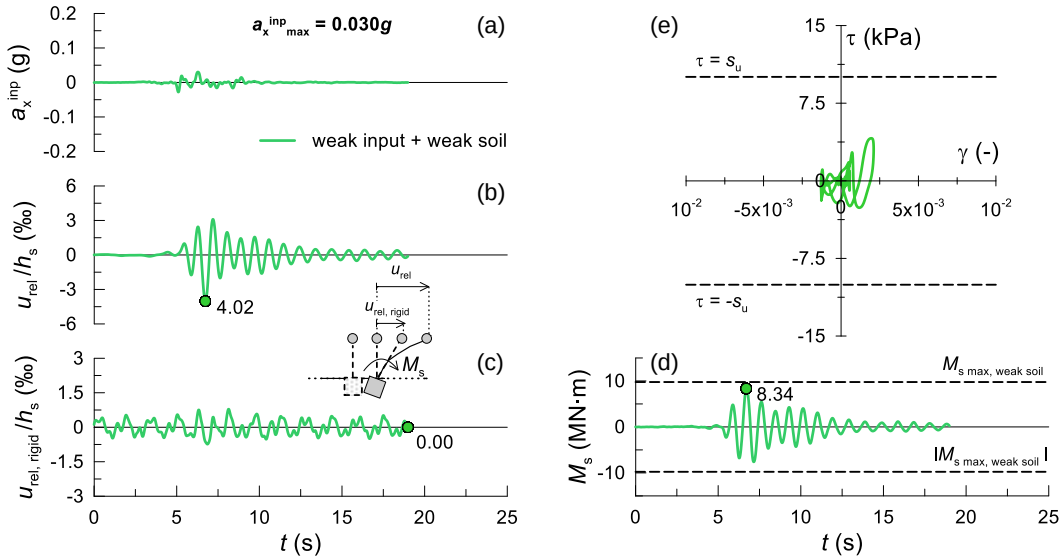

Fig 4. Weak input on weak soil (DG03): (a) applied input; time histories of (b) dimensionless deck drift, (c), rigid rotation and (d) bending moment; (e) free-field shear stress-shear strain loop at depth z = 6.5 m

$$u_{rel} = u_{deck} - u_{caisson\,head} = \tan\theta \cdot h_s + u_{flex} = u_{rel,\,rigid} + u_{flex} \quad (1)$$

where u_{deck} and $u_{caisson\,head}$ are the horizontal displacements of the deck and the top of the caisson, θ is the rigid caisson rotation, $u_{rel,\,rigid}$ is the rigid component of the drift and u_{flex} is the flexural displacement of the pier, that is the one directly related to the bending moment M_s (the latter not shown in this paper for the sake of space). The horizontal displacement time histories were computed by integrating twice the average acceleration time histories obtained from *MEMS* $M_{1\text{-}2}$ and $M_{5\text{-}6}$, while the time history of the rigid rotation θ was computed as $\theta = [w_{L3} – w_{L2}]/d$, where w indicates settlement and d is the distance between *LVDTs* $L_{2\text{-}3}$. The bending moment M_s was obtained as $M_s = m_{eff} \cdot a_x \cdot g \cdot h_s$, where m_{eff} is the effective mass related to the first vibration mode of the pier, a_x is the average horizontal acceleration recorded at the brass mass, g is the gravitational acceleration and h_s is the pier height. All results presented hereafter are at prototype scale, unless otherwise specified.

The observed time histories of drift and bending moment are plotted in Figs. 4, 5, and 6 for the three increasing amplitudes of the ground motion. In the weak input on weak soil case (Fig. 4), no permanent drift is obtained ($u_{rel,\,rigid}/h_s = 0$) due to the very low intensity of the input motion. This result is consistent with the *far-field* shear stress-shear strain loop computed at a depth z = 6.5 m (Fig. 4e), intermediate between piezo-electric accelerometers p_2 and p_3. In this case the maximum shear stress is well below the undrained shear strength of the soil, $s_u \approx 10.0$ kPa, and the stress-strain loop is characterised by quite a narrow area (*i.e.*, small hysteretic damping ratio). This outcome allows to state that the soil behaved almost elastically when subjected to the weak ground motion.

With increasing seismic amplitude, the system starts to accumulate a permanent rigid rotation (Fig. 5c). However, this is still relatively small ($u_{rel,\,rigid}/h_s$ = -0.18 ‰) as a consequence of the higher undrained shear strength measured along the *far-field* alignment at a depth z = 6.5 m, $s_u \approx 41.7$ kPa. Hence, in this test, irreversible soil behaviour influenced the system response only very slightly, while still limiting the inertial forces transmitted to the superstructure; indeed, despite the input amplitude increased more than three times (ratio between $a_x^{inp}{}_{max}$ equal to 0.102/0.030 = 3.4), the increment obtained in the peak values of the deck drift, u_{rel}, was only 33 % and the maximum bending moment, M_s, increased by 72 %. As a further prove that the system performance was governed mainly by the nearly elastic soil behaviour, the frequency contents of the time histories shown in Fig. 5 are very similar to those obtained in Fig. 4.

Conversely, in the case of the strong seismic input applied to the weak soil, the soil shear strength is mobilised, as shown in Fig. 6e. The area of the shear stress-shear strain loop is also significantly

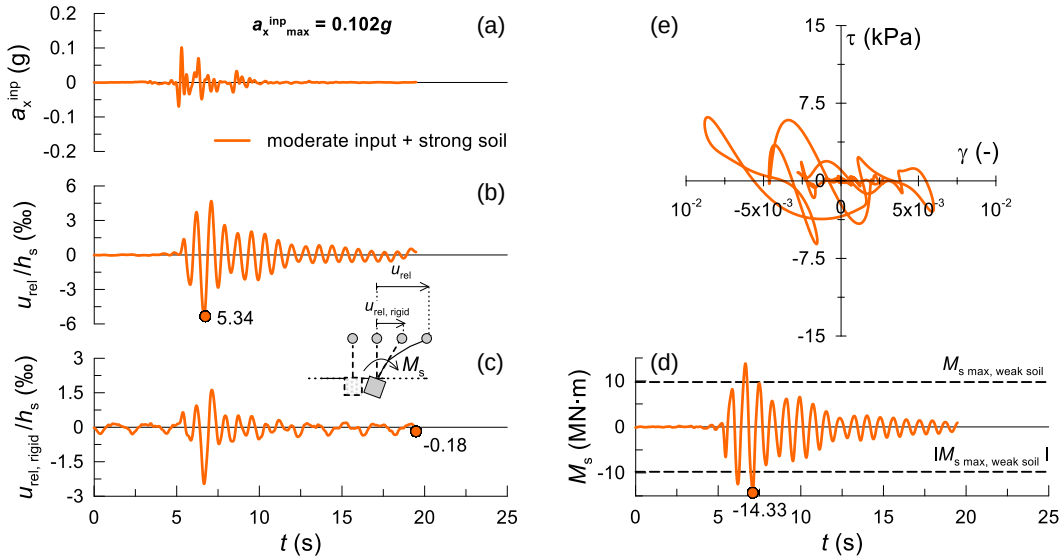

Fig 5. Moderate input on strong soil (DG01): (a) applied input; time histories of (b) dimensionless deck drift, (c), rigid rotation and (d) bending moment; (e) free-field shear stress-shear strain loop at depth z = 6.5 m

larger, indicating that a significant hysteretic damping is developed in the soil deposit. This outcome is consistent with the strong increase of the permanent rotation accumulated by the system, which is tripled (= 0.60 ‰, Fig. 6c). Furthermore, the peak deck drift and the bending moment turned out to be lower than those attained by the moderate input on the strong soil case (Fig. 5); this is apparent for the bending moment, which decreased by about 32 %, despite the input amplitude doubled. The peak bending moment attained in this case ($M_{s\ max,\ weak\ soil}$ = 9.76 MN·m) is also indicated with dashed lines in Figs. 4-6 showing the bending moment time histories. This value might be considered as the moment capacity of the foundation under the weight of the superstructure. It is therefore apparent that the irreversible and hysteretic soil behaviour is contributing to reduce the inertial forces transmitted to the superstructure, governing the system seismic performance. This is also clear from the noticeable period elongation of both the deck drift and bending moment time histories plotted in Fig. 6.

The experimental results are summarised in Fig. 7, where the selected seismic indexes (*i.e.*, peak values of the pier bending moment, a, and deck drifts, b-c) are plotted as a function of the peak acceleration of the seismic input. Indeed, the peak values increase with the seismic intensity when $a_x^{inp}{}_{max} \leq 0.10g$, while they even decrease for larger acceleration; a monotonic increase of the permanent drift is observed instead.

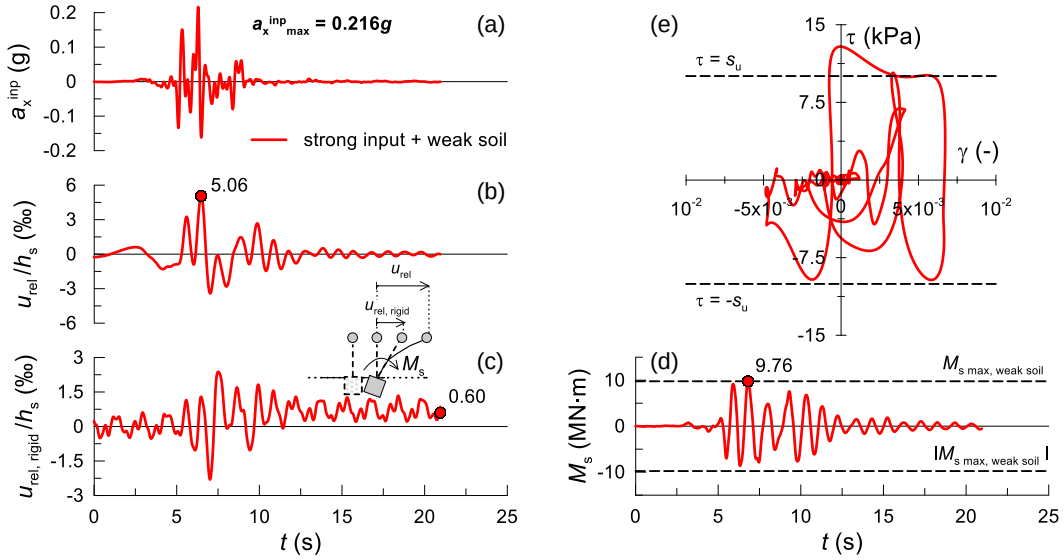

Fig 6. Strong input on weak soil (DG03): (a) applied input; time histories of (b) dimensionless deck drift, (c), rigid rotation and (d) bending moment; (e) free-field shear stress-shear strain loop at depth z = 6.5 m

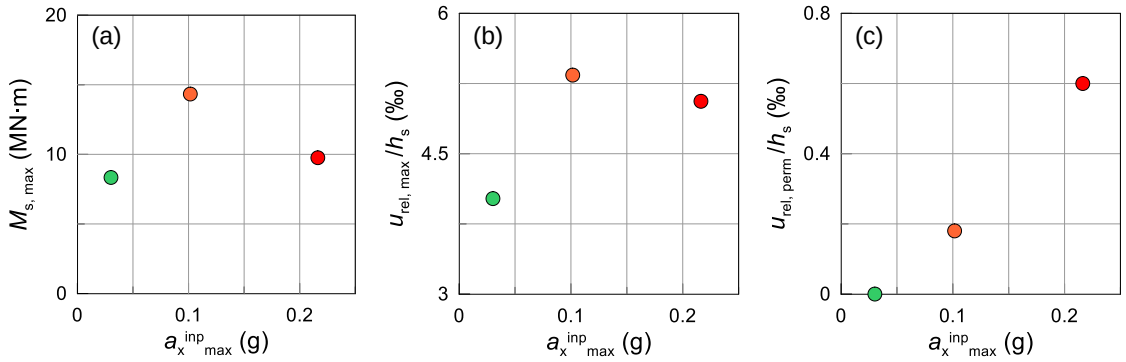

Fig 7. Indexes of the system performance against the peak acceleration of the seismic input: (a) peak bending moment; (b) peak and (c) permanent dimensionless deck drift

4. Concluding remarks and further developments

This paper illustrated a preliminary interpretation of the results obtained from dynamic centrifuge tests of caisson foundations supporting bridge piers subjected to weak, moderate and strong ground motions. The discussion mainly showed that the inelastic and hysteretic behaviour of the soil can play a fundamental role in the system seismic performance; this is particularly true for strong seismic events, for which the soil acts as a "fuse", thus limiting the inertial forces transmitted to the superstructure.

Further elaboration of the discussed results is of course needed, *e.g.*, to understand and quantify the relative contribution of the free-field and near-field hysteretic soil behaviour, considering also the remaining seismic inputs applied in the centrifuge tests. Moreover, the seismic performance of a flexible system resting on an "elastic" soil deposit has been also assessed through centrifuge tests (DG02), highlighting the role of system flexibility on its seismic performance.

References

Brennan A.J., Madabhushi S.P.G. (2002). Design and performance of a new deep model container for dynamic centrifuge testing. Proc. Int. Conf. on Physical Modelling in Geotechnics, Balkema, Rotterdam, The Netherlands, St Johns NF, Canada, 183-188.

Garala T.K., Madabhushi S.P.G. (2019). Seismic behaviour of soft clay and its influence on the response of friction pile foundations. *Bulletin of Earthquake Engineering*, **17**(4), 1919-1939.

Gaudio D., Rampello S. (2019). The influence of soil plasticity on the seismic performance of bridge piers on caisson foundations. *Soil Dynamics and Earthquake Engineering*, **118**, 120-133. DOI: https://doi.org/10.1016/j.soildyn.2018.12.007

Gaudio D., Rampello S. (2021). On the assessment of seismic performance of bridge piers on caisson foundations subjected to strong ground motions. *Earthquake Engineering & Structural Dynamics*, **50**(5), 1429-1450. DOI: https://doi.org/10.1002/eqe.3407

Gazetas G. (2015). 4th Ishihara lecture: soil–foundation–structure systems beyond conventional seismic failure thresholds. *Soil Dynamics and Earthquake Engineering*, 68, 23-39.

Madabhushi S.P.G., Haigh S.K., Houghton N.E., Gould E. (2012). Development of a Servo-Hydraulic Earthquake Actuator for the Cambridge Turner Beam Centrifuge. *International Journal of Physical Modelling in Geotechnics*, **12**(2), 77-88.

Sakellariadis L., Anastasopoulos I., Gazetas G. (2020). Fukae bridge collapse (Kobe 1995) revisited: New insights. *Soils and Foundations*, **60**(6), 1450-1467.